ACES Asian Chemical Editorial Society

DOI: 10.1002/asia.201500847

CHEMISTRY AN ASIAN JOURNAL Full Paper

Drug Delivery

Thermo/pH Dual Responsive Mixed-Shell Polymeric Micelles Based on the Complementary Multiple Hydrogen Bonds for Drug Delivery

Qiuhua Wu, Xiuping Tang, Xue Liu, Yu Hou, He Li, Chen Yang, Jie Yi, Ximing Song, and Guolin Zhang*[a]

Abstract: Thermo/pH dual responsive mixed-shell polymeric micelles based on multiple hydrogen bonding were prepared by self-assembly of diaminotriazine-terminated poly(ε-caprolactone) (DAT-PCL), uracil-terminated methoxy poly(ethylene glycol) (MPEG-U), and uracil-terminated poly(N-vinylcaprolactam) (PNVCL-U) at room temperature. PCL acted as the core and MPEG/PNVCL as the mixed shell. Increasing the temperature, PNVCL collapsed and enclosed the PCL core, while MPEG penetrated through the PNVCL shell, thereby leading to the formation of MPEG channels on the micelles surface. The low cytotoxicity of the mixed micelles was confirmed by an MTT assay against BGC-823 cells. Studies on the in vitro drug release showed that a much faster release rate was observed at pH 5.0 compared to physiological pH, owing to the dissociation of hydrogen bonds. Therefore, the mixed-shell polymeric micelles would be very promising candidates in drug delivery systems.

Introduction

Polymeric micelles self-assembled from amphiphilic copolymers in water have been extensively exploited to improve conventional therapy in drug delivery systems in recent years[1] owing to their capability to increase the solubility and stability of insoluble drugs as well as their good biocompatibility.[2] Micelles generally exhibit a core–shell structure with a hydrophobic inner core as a depot for hydrophobic drugs and a hydrophilic outer shell as a protective interface between the hydrophobic core and external aqueous milieu.[3] However, polymeric micelles become thermodynamically unstable when they are diluted below the critical micelle concentration (CMC) after intravenous injection.[4] The disruption of micellar structures might lead to the burst release of physically encapsulated drugs, which may cause serious side-effects, mostly due to large fluctuations in the drug concentration.[4b] All these characteristics may reduce the effectiveness of drug delivery and limit the in vivo application of polymeric micelles. Several strategies have been developed to solve this stability problem.[5]

Core—shell–corona micelles with three-layered structures are a rational alternative.[4a,6] Core—shell–corona micelles are usually prepared from either a ABC triblock copolymer or two diblock copolymers AB and BC or AB and CD.[7] Compared to the triblock copolymer, the structures of complex micelles formed by two different diblock copolymers are tunable conveniently, because the ratio of the shell and corona can be adjusted by the relative content of the two diblock copolymers.[6b] A key advantage of core—shell–corona micelles is that channels can be created in the shell,[8] which could be applied to suppress burst drug release. For example, Li et al.[9] prepared double-responsive complex micelles by self-assembly of poly(tert-butyl acrylate)-*block*-poly(N-isopropylacrylamide) (P*t*BA-*b*-PNIPAM) and poly(tert-butyl acrylate)-*block*-poly(4-vinylpyridine) (P*t*BA-*b*-P4VP) with a P*t*BA core and a mixed P4VP/PNIPAM shell at room temperature. When the solution temperature or pH value were changed, the PNIPAM or P4VP will collapse on the P*t*BA nuclear, while the P4VP or PNIPAM stretched out still exhibition in solution, formed a kind of adjustable hydrophilic "channel".

Considering the tumor targeting drug delivery field, an ideal anticancer drug carrier should retain the drug molecules in the micellar core in the bloodstream and normal tissues and release them at the specific tumor sites.[4b,10] Hence, incorporation of pH-responsive character into amphiphilic polymers is highly desirable for their potential application as carriers for anticancer hydrophobic drugs because the tumor extracellular environment is more acidic (pH 6.5) than blood and normal tissues (pH 7.4), and the pH values of endosomes and lysosomes are even lower (pH 5–5.5).[1f,3c,11] To date, various pH-responsive polymer micelles based on acid-sensitive groups have been

[a] *Q. Wu, X. Tang, Dr. X. Liu, Y. Hou, H. Li, C. Yang, J. Yi, Prof. X. Song, Prof. G. Zhang*
Liaoning Province Key Laboratory for Green Synthesis and Preparative Chemistry of Advanced Materials
College of Chemistry
Liaoning University
No.66 Chongshan Mid-Road, Huanggu District, Shenyang 110036, Liaoning Province (P. R. China)
Fax: (+86) 24-62202380
E-mail: glzhang@lnu.edu.cn

Supporting information for this article is available on the WWW under http://dx.doi.org/10.1002/asia.201500847.

developed for pH-triggered drug delivery.[10a,12] Compared to conventional covalent-linked polymers, supramolecular polymers based on noncovalent interactions have been found to be more sensitive to external stimuli, which offer a new route for design of drug delivery systems with rapid response abilities.[13] Among various noncovalent interactions, hydrogen bonding is very sensitive to pH variation.[14,13b] For example, Wang et al.[15] prepared the supramolecular amphiphilic block copolymers based on multiple hydrogen-bonding interactions between adenine-terminated poly(ε-caprolactone) (PCL-A) and uracil-terminated poly(ethylene glycol) (PEG-U). Doxorubicin (DOX) was loaded in the PCL core as a model drug. The result showed that the release rate of DOX from micelles at pH 5.0 was remarkably faster than at pH 7.4.

Herein, we benefited from the core—shell–corona three-layered structure and hydrogen bonds connection, and have reported mixed-shell polymeric micelles prepared by self-assembly of diamino-triazine-terminated poly(ε-caprolactone) (DAT-PCL), uracil-terminated methoxy poly(ethylene glycol) (MPEG-U), and uracil-terminated poly(N-vinylcaprolactam) (PNVCL-U) in aqueous solution with a PCL core and a mixed MPEG/PNVCL shell at room temperature. PNVCL, one of the well-known thermosensitive polymers, showed a temperature induced collapse from an extended coil to a globular structure in aqueous solution at 32 °C, called the lower critical solution temperature (LCST). DAT-PCL could assemble into micelles with MPEG-U or PNVCL-U, while MPEG-U···DAT-PCL micelles disintegrated when they were diluted in the blood stream and PNVCL-U···DAT-PCL micelles precipitated above the LCST of PNVCL (after intravenous injection at around 37 °C). As for the mixed micelles, the collapsed PNVCL shell could form hydrophobic domains on the PCL core. The corona formed by the water soluble MPEG chains embedded into the PNVCL shell and acted as a channel and a protective barrier against aggregation of the micelles themselves (Scheme 1).

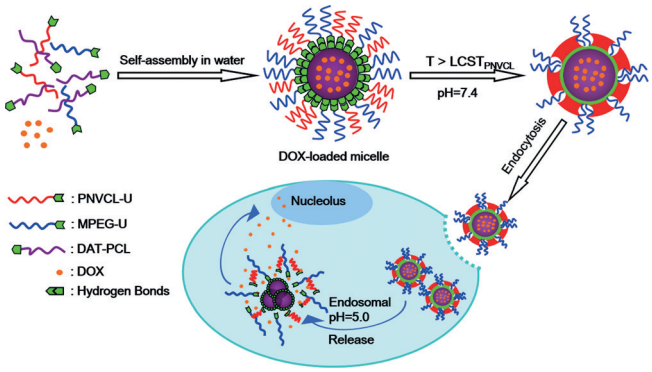

Scheme 1. Schematic representation of the structure and functioning mechanism of DOX-loaded mixed shell micelle.

The micelles remained to protect drug molecules in the bloodstream and normal tissues and released the drug at the specific tumor sites (pH 5.0) due to the disassembly of the micelles by breaking of the hydrogen bonds. The area of the hydrophobic PNVCL domain and MPEG channel could be finely tuned by controlling the relative content of PNVCL and MPEG in the mixed shell. The mixed micelles are promising materials in the site-specific drug delivery system with advantages of high therapeutic effectiveness and minimal side effects of cancer chemotherapy.

Results and Discussion

Synthesis of DAT-PCL and PNVCL-U

The ^{1}H NMR spectrum of the DAT-PCL is shown in Figure S1 (see the Supporting Information). The peaks at 1.39, 1.66, 2.31, and 4.07 ppm are assigned to protons g, f, e, and h in the PCL segments, respectively. The peak at 3.68 ppm is assigned to proton k in the methylene proton conjoint to the end hydroxy group of the PCL unit of the polymer. The peaks at 2.78, 2.98, 4.28, and 5.23 ppm are assigned to protons c, b, d, and a in the DAT segments, respectively. The ^{13}C NMR (300 MHz, $CDCl_3$) spectrum of the DAT-PCL is shown in Figure S2 (see the Supporting Information). The ^{13}C NMR results further demonstrate the successful grafting of DAT on PCL. The FTIR spectrum of DAT-PCL is shown in Figure S3 (see the Supporting Information).

The ^{1}H NMR spectrum of the PNVCL-U is shown in Figure S4 (see the Supporting Information). The peaks at 1.14–2.0, 2.5, 3.2, and 4.4 ppm are assigned to protons b + d + e, c, f, and a in the PNVCL segments, respectively. The peaks at 3.74, 3.91, and 4.24 ppm are assigned to protons g, i, and h in the $-SCH_2COOCH_2CH_2-$ segments, respectively. The peaks at 5.74, 7.52, and 8.24 ppm are assigned to protons k, j, and l in the uracil segments, respectively. The Figure S5 (see the Supporting Information) is the ^{13}C NMR (300 MHz, $CDCl_3$) spectrum of PNVCL-U. The ^{13}C NMR results further demonstrate the successful grafting of uracil on PNVCL. The FTIR spectra of the PNVCL-U and PNVCL-COOH are shown in Figure S6 (see the Supporting Information).

The GPC traces of polymers are shown in Figure S7 (see the Supporting Information), and all polymers showed the unimodal peak, which further indicated that the polymerization was completed successfully and there was no another polymer in the product. Molecular weights and molecular weight distributions were measured by GPC and summarized in Table 1.

Table 1. Related data on all polymers.

Sample	ε-CL/DAT[a]	M_n[b] [g mol^{-1}]	M_n[c] [g mol^{-1}]	M_w[c] [g mol^{-1}]	PDI[c]
DAT-PCL**1**	30/1	3749	4016	4716	1.17
DAT-PCL**2**	40/1	5694	4823	5221	1.08
DAT-PCL**3**	76/1	9449	8942	9745	1.09
PNVCL-COOH	–	7022	6869	7899	1.15
PNVCL-U	–	7178	6985	8312	1.19
MPEG-U	–	5139	5394	5664	1.05

[a] Molar ratio of DAT to ε-CL in feed. [b] Determined by ^{1}H NMR spectroscopy in $CDCl_3$ solution. [c] Determined by GPC in THF at 30 °C.

Hydrogen Bonding Interactions between DAT-PCL and MPEG-U (or PNVCL-U)

The formation of complementary multiple hydrogen bonds between DAT-PCL and MPEG-U (or PNVCL-U) was analyzed by ^{1}H NMR spectroscopy for the blend of two polymers (DAT-PCL/MPEG-U, 1:1) in $CDCl_3$. Compared with the ^{1}H NMR of DAT-PCL**2** and MPEG-U, typical ^{1}H NMR spectrum of MPEG-U···DAT-PCL**2** (Figure S8A in the Supporting Information) not only reveals signals of the MPEG and PCL block, but also the chemical shift of the NH resonance moving downfield systematically from 8.24 to 10.49 ppm and the NH_2 resonance moving downfield systematically from 5.23 to 5.41 ppm. The results of the ^{1}H NMR spectrum suggest that polymer chains are linked through complementary hydrogen bonds.[16] The ^{1}H NMR spectrum of PNVCL-U···DAT-PCL**2** is shown in Figure S8B (see the Supporting Information) and it also has the same movement in the chemical shift.

To evaluate the hydrogen-bonding interactions, FTIR spectroscopy was performed to examine the hydrogen bonds between DAT-PCL**2** and MPEG-U (or PNVCL-U). The FTIR spectrum of MPEG-U···DAT-PCL**2** is shown in Figure S9A (see the Supporting Information). Figure S9A illustrates the FTIR spectra in the C=O stretching region (1700≈1650 cm^{-1}) of uracil. The C=O stretching peak shifted to a lower frequency with the increased PCL-DAT content, thus indicating the formation of the hydrogen bonds.[17] The FTIR spectrum of PNVCL-U···DAT-PCL**2** is shown in Figure S9B and the peak shift occurs.

Formation of the Micelles and pH-Triggered Destabilization

In this study, all of the micellar solutions have the same polymer concentration of 0.1 mg mL^{-1}. Figure S10 (see the Supporting Information) shows that all of the MPEG-U···DAT-PCL micelles exhibit unimodal size distribution with the mean diameter from 112 to 139 nm. The sizes of micelle increased with an increase in the proportion of hydrophobic segment, so the size of the supramolecular copolymer micelle could be adjusted by changing the proportion of hydrophobic segment.

The morphologies of MSM (MPEG-U···DAT-PCL**2**/PNVCL-U···DAT-PCL**2** (1:1 molar ratio) and MSM-DOX (1:1) visualized by TEM are shown in Figure 1. The MSM and MSM-DOX are all approximate spherical micelles in aqueous solution and the micelle sizes determined by TEM are in accordance with the data from dynamic light scattering (DLS). It can be seen that the hydrodynamic diameter (D_h) of the drug-loaded micelles are slightly larger than that of corresponding blank micelles.

The hydrogen-bonding interactions between the hydrophobic DAT-PCL core and hydrophilic MPEG-U and PNVCL-U shell made mixed-shell polymeric micelles unstable at acidic pH. To evaluate the pH-responsive, the MSM were treated with pH 5.0 acetate buffer (50 mM) and the particle sizes were followed by DLS measurements at different time intervals.

Figure 2A shows that MSM (5:5) aggregate rapidly at pH 5.0. The size of MSM increases from 125 nm to about 685 nm in 4 h, and reaches over 1000 nm after 24 h. Figure 2B shows that the micelle solution becomes turbid at pH 5.0 after 48 h,

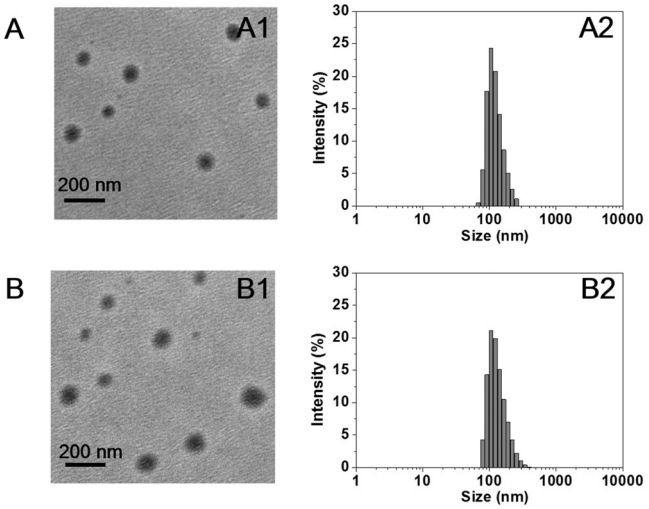

Figure 1. TEM images (left) and DLS studies (right) of MSM (1:1) (A) and MSM-DOX (1:1) (B).

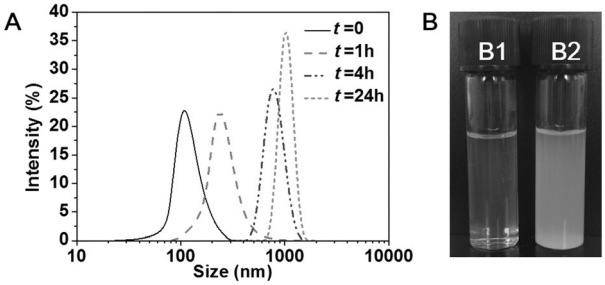

Figure 2. (A) Change in size of MSM (1:1) over time at pH 5.0 at 25 °C monitored by DLS; (B) Photographs of MSM (1:1) over 48 h (B1) pH 7.4, (B2) pH 5.0.

while it remains clear under pH 7.4. The change in micelle size at low pH is attributed to the protonation, which leads to the shedding of the hydrophilic shell from the micelles and the aggregation of the hydrophobic core. In contrast, no change in micelle size is observed after 48 h at pH 7.4.

Drug Loading and Release from the Micelles

Hydrophobic DOX was well encapsulated into the hydrophobic inner cores of the SM and MSM (1:1) with a loading efficiency of about 29.6% and 24.8%, and a loading content of 12.9% and 11.0%, respectively. It should be noted that MSM show a slight increased average size of about 138 nm, as measured by TEM and DLS (see Figure 1B1 and 1B2 in the Supporting Information), wherein the polydispersity of polymeric micelles is fairly low, indicating narrow size distribution. The drug release experiment was performed in acetate buffer solution (pH 5.0, 0.05 M) and in phosphate buffer solution (pH 7.4, 0.05 M), respectively.

Figure 3 shows the DOX release rate of from SM-DOX and MSM-DOX (5:5) at pH 5.0 and pH 7.4 at 37 °C, respectively. It could be seen that for two kinds of micelles the release rate of

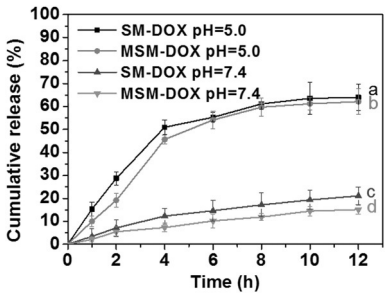

Figure 3. In vitro release profiles of DOX from SM-DOX and MSM-DOX (1:1) at different pH values (a) pH 5.0, (b) pH 7.4 at 37 °C.

DOX at pH 5.0 was faster than that at pH 7.4. This is because DOX is a kind of cationic drug and its solubility in acidic water is good,[8b] and two kinds of micelles are destabilized and shedding of micelle shell under acidic conditions.[15] In addition, the DOX release rate from SM-DOX was faster than the MSM-DOX at 37 °C. This is because the PNVCL chains in MSM could collapse unto the PCL core at 37 °C, which could hinder the release of DOX from the micelles.[8b]

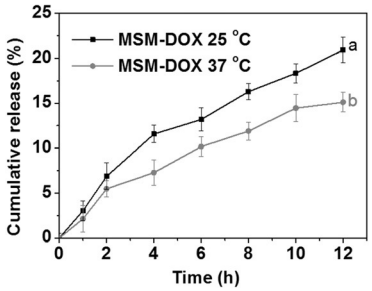

Figure 4. In vitro release profiles of DOX from MSM-DOX (1:1) at different temperatures (a) 25 °C, (b) 37 °C at pH 7.4.

Figure 4 shows the release rate of DOX from MSM-DOX (1:1) at 25 °C and 37 °C at pH 7.4. The drug release rate at 25 °C was faster than at 37 °C. This is because PNVCL is soluble at 25 °C, but is insoluble at 37 °C (see Figure S11 in the Supporting Information) and could collapse into the PCL core (Scheme 1). These results also show that the micelles are markedly thermoresponsive.[8]

Figure 5 shows the release profiles of DOX from MSM-DOX with different ratios of MPEG-U···DAT-PCL**2** to PNVCL-U···DAT-PCL**2** at pH 7.4 at 37 °C, respectively. Obviously, the drug release rate decreased with decreasing ratio of MPEG-U···DAT-PCL**2** to PNVCL-U···DAT-PCL**2**. This was because the area of MPEG channels decreased with decreasing the content of MPEG.

In Vitro Cytotoxicity of the Micelles

The cytotoxicity of SM and MSM were evaluated by MTT assay using BGC-823 cells. Figure 6 shows the cell viability after 48 h of incubation with the micelles of SM and MSM respectively, at

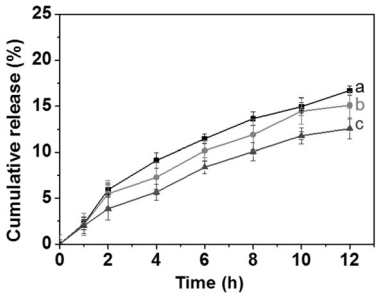

Figure 5. In vitro release profiles of DOX from MSM-DOX at pH 7.4 at 37 °C with different ratios of MPEG-U···DAT-PCL**2** to PNVCL-U···DAT-PCL**2** (a) 3:2 molar ratio, (b) 1:1 molar ratio, (c) 2:3 molar ratio, respectively.

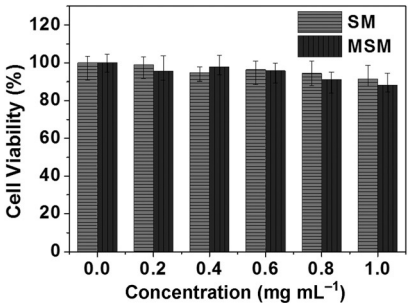

Figure 6. Cytotoxicity of BGC-823 cells against SM and MSM (1:1) after cultured for 48 h with different micelle concentrations.

different concentrations (the total amount of micelles in RPMI-1640 medium).

The results demonstrate that no obvious cytotoxicity against BGC-823cells is observed even if the concentration of copolymer micelles is up to 1.0 mg mL^{-1}. Therefore, these micelles exhibit low cytotoxicity to BGC-823 cells.

In Vitro Cellular Uptake

The cellular uptake and intracellular release behavior of MSM-DOX (1:1) by BGC-823 cells were performed on an inverted fluorescence microscope. As shown in Figure 7, the weaker DOX fluorescence was observed and mainly in the cytoplasm

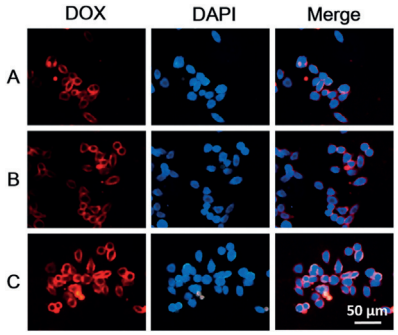

Figure 7. Inverted fluorescent microscopy images of BGC-823 cells after incubation with MSM-DOX (1:1) at pH 7.4 for 2 h (A), 4 h (B) and 12 h (C), respectively. The cell nuclei were stained with DAPI (blue). Scale bar = 50 μm.

of the cells when the cells were cultured in the MSM-DOX for 2 h.

However, the fluorescence remained nearly constant when the cells were cultured in the MSM-DOX for 4 h. After 12 h incubation, much stronger fluorescence of DOX was observed and partly localized in the cell nucleus. As observed in Figure 7A and C, MSM-DOX was internalized through an endocytosis pathway and then the DOX molecules were released and diffused through endocytic compartments to the nucleus eventually.[15]

In Vitro Cytotoxicity of DOX-Loaded Micelles

Figure 8 shows the viability of BGC-823 cells after incubation with SM-DOX, MSM-DOX (1:1), and free DOX at different doses

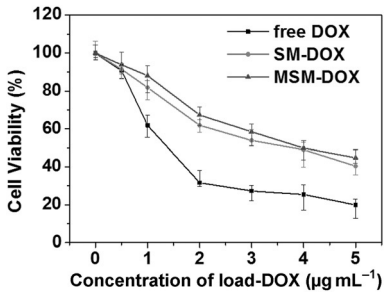

Figure 8. Cytotoxicity of BGC-823 cells against SM-DOX and MSM-DOX (1:1) after cultured for 48 h with different micelle concentrations.

of DOX from 0–5.0 μg mL^{-1}. The IC_{50} value (a concentration at which 50% of cells were killed) for free DOX was 1.3 μg mL^{-1}, while that for SM-DOX and MSM-DOX were 3.8 and 4.3 μg mL^{-1}, respectively. The results demonstrate that DOX-loaded micelles are able to enter the cells and produce the desired pharmacological action. DOX-loaded micelles show a slightly lower cytotoxicity than that of free DOX, which can be attributed to the slow release of DOX from micelles and delay nuclear uptake in BGC-823 cells, as evidenced by the in vivo DOX release.

Conclusions

Stimuli-responsive drug delivery systems that can release drugs in a controllable manner are highly desirable, especially for the delivery of anticancer drugs. We have successfully developed stimuli-responsive mixed shell micelles as a drug nanocarrier. In the first step, MPEG-U, DAT-PCL, and PNVCL-U were synthesized and their self-assembly in solution was studied. In addition, we have demonstrated that the complex micelles have strong response to mild acid pH and are capable of rapidly releasing DOX inside the cells to yield significantly enhanced drug efficacy. The resulting micelles are nontoxic. Importantly, the DOX-loaded micelles could be successfully internalized into cancer cells. These mixed shell micelles based on complementary multiple hydrogen bonds are very appealing drug carriers, because they can potentially combine the advantages of traditional covalent-linked copolymer micelles. Therefore, this type of shell-responsive micelles are very promising candidates for improvements in drug delivery systems.

Experimental Section

Materials

Uracil (≥98.0%), ε-caprolactone (ε-CL), mono-methoxy poly(ethylene glycol) (MPEG) with M_n = 5000 g mol^{-1}, 2-mercaptoethanol, mercapto acetic acid, *N*,*N*-dicyclohexylcarbodiimide (DCC), and 4-dimethylaminopyridine (DMAP) were purchased from Alfa Aesar Co., Ltd. Stannous octoate ($Sn(Oct)_2$), ethylene carbonate, *N*-vinylcaprolactam, azobisisobutyronitrile (AIBN), and 2,2-dimethoxy-2-phenylacetophenone (DMPA) were purchased from Sigma–Aldrich Chemical Reagent Co., Ltd. Doxorubicin hydrochloride (DOX·HCl) was purchased from Adamas Chemical Reagent Co., Ltd. *N*,*N*-Dimethylformamide (DMF), 1,4-dioxane, and dichloromethane (CH_2Cl_2) were purchased from Sinopharm Chemical Reagent Co., Ltd. (Shanghai, China), and dried over calcium hydride for 48 h and then distilled before use. *p*-Toluenesulfonyl chloride (TsCl) was purchased from Sinopharm Chemical Reagent Co., Ltd. (Shanghai, China). A clear polystyrene tissue culture treated 12-well and 96-wellplates were obtained from Beijing Dingguo Changsheng Biotechnology Co., Ltd. Dialysis bag (molecular weight cut off: 1 KD) was obtained from Shanghai Baoman Biological Technology Co., Ltd. All other reagents and solvents were of analytical grade and used as received unless otherwise mentioned.

Synthesis of MPEG-U

MPEG-U was prepared according to the literature.[15] First, MPEG and TsCl reacted to obtain MPEG-sulfanilic acid ester (MPEG-OTs). Then, MPEG-OTs was treated with uracil to give MPEG-U in 82% yield. ^{1}H NMR (300 MHz, $CDCl_3$): δ = 8.27 (s, 1H, -CO***NH***CO-), 7.37 (d, 1H, -N***CH***CH-), 5.65 (d, 1H, -CH***CH***CO-), 3.92 (t, 2H, -CH_2***CH_2***N-), 3.65–3.74 (m, 4H, -O***CH_2CH_2***-,), 3.54 ppm (s, 3H, ***CH_3***OCH_2-). ^{13}C NMR (300 MHz, [D_6]DMSO): δ = 47.14 (-CH_2***C***H_2N-), 58.02 (***C***H_3O-), 67.84 (-***C***H_2CH_2N-), 69.72 (-***C***H_2***C***H_2O-), 71.31 (CH_3O***C***H_2-), 102.12 (-CH***C***HCO-), 146.31 (-***C***HCHCO-), 150.11 (-N***C***ONH-), 167.32 ppm (-CH***C***ONH-).

Synthesis of Diaminotriazine (DAT)

A mixture containing 2,4-diamino-6-vinyl-s-triazine (4.11 g, 0.03 mol), DMPA (0.380 g, 0.0015 mol), and 2-mercaptoethanol (4.4 mL, 0.06 mol) in DMF (100 mL) was irradiated by UV at 365 nm for 1 h. The DMF was removed under reduced pressure and the product was washed with a mixture of acetone and ethanol (80 mL, v/v = 1:1) three times to give a white powder in 55% yield. The ^{1}H NMR spectrum of the DAT is shown in Figure S12. ^{1}H NMR (300 MHz, [D_6]DMSO): δ = 6.63 (s, 4H, -***NH_2***), 2.82 (t, 2H, -***CH_2***CH_2S-), 2.57 (t, 4H, -***CH_2SCH_2***-), 3.51 (q, 2H, -***CH_2***OH), 4.80 ppm (s, 1H, -***OH***), MS (Bruker Reflex III time-of-flight mass spectrometer) *m*/*z*: calcd. for $C_7H_{13}N_5OS$ 215.27; found 216.00. The ^{13}C NMR and FTIR spectra (300 MHz, [D_6]DMSO) of DAT are shown in Figure S13 and Figure S14 in the Supporting Information, respectively.

Synthesis of DAT-PCL

DAT-PCL was synthesized by ring-opening polymerization of ε-CL initiated by DAT with $Sn(Oct)_2$ as a catalyst. The necessary amounts of DAT, ε-CL, and $Sn(Oct)_2$ were added into a 50 mL round flask followed by six cycles of evacuation-purging with purified nitrogen.

The polymerization reaction was performed in an oil bath at 120 °C and terminated after 24 h under stirring. After being cooled to room temperature, the resulting polymer was dissolved in CH_2Cl_2 and precipitated in diethylether three times. The precipitate was dried in vacuum at 25 °C for 24 h to give the desired DAT-PCL polymers as a white solid. The yield was approximately 65%. The reaction route is shown in Scheme 2. Different molar ratios of the feeding ε-CL to DAT resulted in the corresponding polymers with various compositions as listed in Table 1.

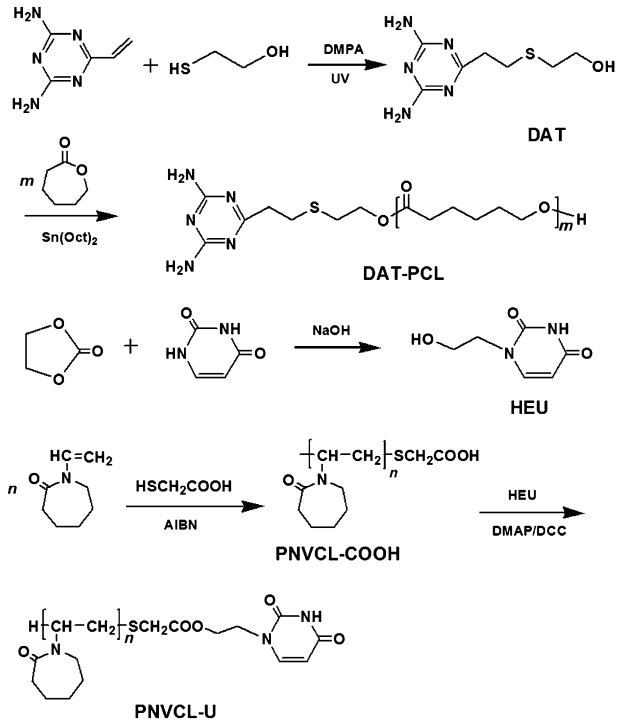

Scheme 2. The synthetic routes for DAT-PCL and PNVCL-U.

Synthesis of 1-(2-Hydroxyethyl) Uracil (HEU)

A mixture containing uracil (1.121 g, 0.01 mol), ethylene carbonate (0.969 g, 0.011 mol), and NaOH (0.02 g, 0.5 mmol) in DMF (60 mL) was maintained at 160 °C for 1.5 h. The DMF was removed under reduced pressure and the residue was recrystallized from 1,4-dioxane (30 mL) three times to give a white powder in 29% yield. MS (Bruker Reflex III time-of-flight mass spectrometer) *m/z*: calcd. for $C_6H_8N_2O_3$ 156.14; found 156.90. The ^{1}H NMR spectrum of the HEU is shown in Figure S15 in the Supporting Information. ^{1}H NMR (300 MHz, [D$_6$]DMSO): $\delta = 8.50$ (s, 1H, -CO***NH***CO-), 7.40 (d, 1H, -CO***CH***=CH-), 5.44 (d, 1H, -CH=***CH***N-), 3.58–3.37 ppm (m, 5H, -***CH$_2$CH$_2$OH***). The ^{13}C NMR (300 MHz, [D$_6$]DMSO) and FTIR spectra of HEU are shown in Figure S16 and Figure S17 in the Supporting Information, respectively.

Synthesis of PNVCL-U

NVCL (2.5020 g, 18 mmol) and AIBN (0.0405 g, 0.2475 mmol) were dissolved in 1,4-dioxane (10 mL) and nitrogen was bubbled through the solution for 30 min. Then, mercapto acetic acid (0.0331 g, 0.36 mmol) was dissolved in 1,4-dioxane (2.0 mL) and added into the reactor. The polymerization was performed at 68 °C under stirring and terminated after 12 h. After being cooled to room temperature and removal of 1,4-dioxane under reduced pressure, the resulting polymer was dissolved in dichloromethane (20 mL) and precipitated in *n*-hexane (500 mL) three times. The precipitate was dried in vacuum at 25 °C for 24 h to give the desired PNVCL-COOH as a white solid in 70% yield. ^{1}H NMR (300 MHz, $CDCl_3$): $\delta = 4.65$–4.25 (m, 1H, -***CH***CH_2SCH_2-), 2.45–2.62 (t, 2H, -***CH$_2$***CON-), 3.01–3.45 (m, 2H, -CON***CH$_2$***-), 3.74 (s, 2H, -S***CH$_2$***COOH), 1.18–2.02 ppm (m, 8H, -CH_2***CH$_2$CH$_2$CH$_2$***CH_2NCH***CH$_2$***-).

PNVCL-COOH (1.4084 g, 0.2 mmol), DMAP (0.0068 g, 0.056 mmol), and DCC (0.1154 g (0.56 mmol) were dissolved in DMF (10 mL) and nitrogen was bubbled through the solution for 30 min. Then, 1-(2-hydroxyethyl) uracil (0.312 g, 2.0 mmol) was dissolved in DMF (2.0 mL) and added into the reactor. The reaction was performed at 25 °C under stirring and terminated after 24 h. After removal of DMF under reduced pressure, the resulting polymer was dissolved in ethyl acetate (50 mL). After filtration, the ethyl acetate was removed under reduced pressure and the product was dissolved in acetone (10 mL) and precipitated in *n*-hexane (350 mL) three times. The precipitate was dried in vacuum at 25 °C for 24 h to give the desired PNVCL-U as a white solid in 54% yield. The reaction route is shown in Scheme 2.

Preparation of Micelles

DAT-PCL, MPEG-U, and PNVCL-U (2:1:1 molar ratio) were first dissolved in DMF, respectively, to give the original solution of polymers with a concentration of 1.0 mg mL^{-1}. For preparation of a specific micelle, an original solution of different polymers was mixed together, and then the solution was added dropwise into a given amount of ultra-purified water under vigorous stirring until opalescence appeared. The solution stirred overnight and then dialyzed against water to remove DMF. The single micelle (SM) was prepared only with MPEG-U and DAT-PCL, while the mixed shell micelle (MSM) composed of MPEG and PNVCL segment on the surface of the PCL core was prepared with the mixture of MPEG-U···DAT-PCL and PNVCL-U···DAT-PCL micelle solution. The yields of SM and MSM (1:1) were 92% and 94% (weight of resulting micelles/weight of copolymers in feed), respectively.

Preparation of DOX-Loaded Micelles

Drug-loaded micelles, SM-DOX and MSM-DOX were prepared by adding the polymer and DOX solution into ultra-purified water under vigorous stirring until opalescence appeared, indicating the formation of micelles. The solution was stirred overnight and then dialyzed against water to remove DMF. Finally, the micelle solution was filtered through a 0.45 μm Millipore filter to remove unencapsulated drug particles. For determination of drug loading content, the DOX-loaded micelle solution was lyophilized and then dissolved in DMF. The UV absorbance at 485 nm was measured to determine the DOX concentration.

Drug loading content (DLC) and drug loading efficiency (DLE) were calculated according to the following formulae [Eq. (1) and (2)]:

$$\mathrm{DLC}(\%) = \frac{\text{weight of loaded drug}}{\text{total weight of polymer and loaded drug}} \times 100\% \quad (1)$$

$$\mathrm{DLE}(\%) = \frac{\text{weight of loaded drug}}{\text{total weight of drug in feed}} \times 100\% \quad (2)$$

In Vitro Release Study

The drug release experiment was performed in acetate buffer solution (pH 5.0, 0.05 M) and in phosphate buffer solution (pH 7.4,

0.05 M), respectively. Briefly, 6.0 mL of micelle solution was transferred into a dialysis bag, and then the bag was immersed in 14 mL of buffer solution at 37 °C. Periodically, 4.0 mL of the solution outside the dialysis bag (V_e) was taken out for UV/Vis measurements. The volume of solution was kept constantly by adding 4.0 mL of original buffer solution after each sampling. The amount of drug was measured using a UV/Vis spectrophotometer at 485 nm for DOX. The cumulative percent drug release (E_r) was calculated based on Equation (3).

$$E_r(\%) = \frac{V_e \sum_1^{n-1} C_i + V_0 C_n}{m_{DOX}} \times 100\% \quad (3)$$

E_r: the total cumulative release % of DOX; V_e: the replacement of PBS volume (4.0 mL); V_0: the total amount of PBS volume (14 mL); C_i: DOX concentration of the i-th ($i = 1, 2, 3, 4, 5, 6, 7$) replacement liquid (μg mL^{-1}) (determined by UV/Vis spectrophotometer measurement); C_n: DOX concentration of the last replacement liquid (μg mL^{-1}); m_{DOX}: the total amount of DOX in micelle (μg). The in vitro release experiments were carried out in triplicate at each pH to get the final release curves.

Cytotoxicity Measurements of Blank Micelles

The cytotoxicity of the blank micelles was examined by MTT assay. All sample solutions were diluted with RPMI-1640 medium to obtain preset concentrations. BGC-823 cells were seeded into 96-well plates at a density of 1×10^5 cells per well in 100 μL RPMI-1640 for 24 h. The medium was then replaced with 100 mL of sample solutions in RPMI-1640. The cells were grown for another 48 h. Then, 20 μL of a 5.0 mg mL^{-1} MTT assays stock solution in PBS was added to each well. After incubating the cells for 4 h, the medium containing MTT was removed and 120 μL of DMSO was added to each well to dissolve the MTT formazan crystals. Finally, the plates were shaken for 10 min, and the absorbance of formazan product was measured at 492 nm using a microplate reader (Bio-Rad 680, America).

In Vitro Cellular Uptake

The cellular uptake experiments were performed on an inverted fluorescence microscope. BGC-823 cells were seeded into 12-well plates at a density of 1×10^5 cells per well in 500 μL RPMI-1640 medium/PBS. After an incubation of 24 h, the culture medium of each well was replaced with 500 μL of fresh medium that contained MSM-DOX (10 μg mL^{-1} equivalent DOX concentration) for 4, 6 or 12 h. After the preset time intervals, the culture medium was removed. Cells were washed with PBS buffer (3×500 μL), and then they were stained with DAPI to visualize the nucleus and observed with an inverted fluorescence microscope.

Activity Analyses

The cytotoxicity of free DOX and MSM-DOX against BGC-823 cells was evaluated in vitro by the MTT assay. In the MTT assay, BGC-823 cells were seeded into 96-well plates with a density of 1×10^5 cells per well and incubated in RPMI-1640 (100 μL) for 24 h. The medium was then replaced with 100 mL of serial dilutions of free DOX or MSM-DOX solutions in RPMI-1640. The cells were grown for another 48 h. Then, 20 μL of a 5.0 mg mL^{-1} MTT assay stock solution in PBS was added to each well. After incubating the cells for 4 h, the medium containing MTT was removed and DMSO (120 μL) was added to each well to dissolve the MTT formazan crystals. Finally, the plates were shaken for 10 min, and the absorbance of formazan product was measured at 492 nm using a Bio-Rad 680 microplate reader.

Characterizations

The FTIR spectra were collected by a PerkinElmer FTIR spectrometer using KBr disks. ^{1}H NMR and ^{13}C NMR spectra were measured on a Varian Mercury-300 NMR spectrometer at room temperature, using $CDCl_3$ (or [D_6]DMSO) as a solvent. Chemical shifts (δ) were given in ppm using tetramethylsilane (TMS) as an internal reference. The mass spectra (MS) were measured on Bruker Reflex III time-of-flight mass spectrometer. The gel permeation chromatography (GPC) measurement was conducted with a Waters 1515 GPC instrument equipped with a HT4 and HT3 column (effective molecular-weight range: 5000 to 600 000 and 500 to 30 000) and a 2414 differential refractive index detector. THF was used as an eluent with the flow rate of 1.0 mL min^{-1} at 30 °C and the molecular weights were calibrated with polystyrene standards. The size distribution of micelles was determined by DLS using a Malvern Nano ZS instrument. Transmission electron microscopy (TEM) measurements were conducted using a Hitachi H-7650 electron microscope at an acceleration voltage of 80 kV. To prepare the TEM samples, the sample solution was dropped onto a carbon-coated copper grid and dried slowly in air. UV/Vis was measured on a Purkinje General TU-1900 UV/Vis spectrophotometer at room temperature. The cellular uptake was observed with an Olympus CKX41 inverted fluorescence microscope. The lower critical solution temperature (LCST) of the aqueous solution of the PNVCL-U was investigated on a Purkinje General TU-1900 UV/Vis spectrophotometer together with a NESLAB RTE-111 temperature controller. Briefly, the polymers were dispersed in ultra purified water (Aquaplus 18.2 MΩ). The transmittance of aqueous solutions of polymer at $\lambda = 500$ nm was recorded in a 1.0 cm path length quartz cell. In the heating-cooling cycle, the rate of heating or cooling was set at 1 °C min^{-1} with hold steps of 10 min at each temperature. Values for the LCST of aqueous solutions of the polymers were determined at a temperature with a half of the optical transmittance between blow and above transitions.

Acknowledgements

This work was financially supported by the Natural Science Foundation of China (No. 51373073 and 51403093) and the Natural Science Foundation for Education Department of Liaoning Province of China (No. L2012007).

Keywords: Core—shell–corona structures · drug delivery · hydrogen bonds · polymeric micelles · thermo/pH dual responsive

[1] a) J. J. Chen, J. X. Ding, Y. Zhang, C. S. Xiao, X. L. Zhuang, X. S. Chen, *Polym. Chem.* **2015**, *6*, 397–405; b) K. Kataoka, T. Matsumoto, M. Yokoyama, T. Okano, Y. Sakurai, S. Fukushima, K. Okamoto, G. S. Kwon, *J. Controlled Release* **2000**, *64*, 143–153; c) Z. K. Zhang, R. J. Ma, L. Q. Shi, *Acc. Chem. Res.* **2014**, *47*, 1426–1437; d) A. Lavasanifar, J. Samuel, G. S. Kwon, *Adv. Drug Delivery Rev.* **2002**, *54*, 169–190; e) J. Du, S. P. Armes, *J. Am. Chem. Soc.* **2005**, *127*, 12800–12801; f) B. Yang, Y. Lv, J. Y. Zhu, Y. T. Han, H. Z. Jia, W. H. Chen, J. Feng, X. Z. Zhang, R. X. Zhuo, *Acta Biomater.* **2014**, *10*, 3686–3695; g) I. Choi, S. T. Malak, W. N. Xu, W. T. Heller, C. Tsitsilianis, V. V. Tsukruk, *Macromolecules* **2013**, *46*, 1425–1436.

[2] a) S. Kim, J. Tan, F. Nederberg, K. Fukushima, Y. Yang, R. Waymouth, J. Hedrick, *Macromolecules* **2009**, *42*, 25–29; b) M. W. Amjad, M. C. I. M.

Amin, H. Katas, A. M. Butt, *Nanoscale Res. Lett.* **2012**, *7*, 687; c) Z. L. Tyrrell, Y. Q. Shen, M. Radosz, *Prog. Polym. Sci.* **2010**, *35*, 1128 – 1143.
[3] a) K. Letchford, R. Liggins, K. M. Wasan, H. Burt, *Eur. J. Pharm. Biopharm.* **2009**, *71*, 196 – 206; b) J. L. Yan, Z. Y. Ye, M. Chen, Z. Z. Liu, Y. Xiao, Y. Zhang, W. S. Tan, M. D. Lang, *Biomacromolecules* **2011**, *12*, 2562 – 2572; c) A. Car, P. Baumann, J. T. Duskey, M. Chami, N. Bruns, W. Meier, *Biomacromolecules* **2014**, *15*, 3235 – 3245.
[4] a) C. L. Lo, S. J. Lin, H. C. Tsai, W. H. Chan, C. H. Tsai, C. D. Cheng, G. H. Hsiue, *Biomaterials* **2009**, *30*, 3961 – 3970; b) Y. Q. Yang, B. Zhao, Z. D. Li, W. J. Lin, C. Y. Zhang, X. D. Guo, J. F. Wang, L. J. Zhang, *Acta Biomater.* **2013**, *9*, 7679 – 7690.
[5] a) N. Kang, M. E. Perron, R. E. Prud'Homme, Y. Zhang, G. Gaucher, J. C. Leroux, *Nano Lett.* **2005**, *5*, 315 – 319; b) C. L. Lo, K. M. Lin, C. K. Huang, G. H. Hsiue, *Adv. Funct. Mater.* **2006**, *16*, 2309 – 2316; c) C. L. Lo, C. K. Huang, K. M. Lin, G. H. Hsiue, *Biomaterials* **2007**, *28*, 1225 – 1235.
[6] a) Y. Luo, J. Yuan, X. Liu, H. Xie, Q. Gao, *J. Bioact. Compat. Polym.* **2010**, *25*, 292 – 304; b) C. L. Wu, R. J. Ma, H. He, L. Z. Zhao, H. J. Gao, Y. L. An, L. Q. Shi, *Macromol. Biosci.* **2009**, *9*, 1185 – 1193; c) I. K. Voets, A. De Keizer, M. A. Cohen Stuart, P. De Waard, *Macromolecules* **2006**, *39*, 5952 – 5955; d) S. De Santis, R. D. Ladogana, M. Diociaiuti, G. Masci, *Macromolecules* **2010**, *43*, 1992 – 2001.
[7] P. Petrov, C. B. Tsvetanov, R. Jérome, *J. Phys. Chem. B* **2009**, *113*, 7527 – 7533.
[8] a) X. Liu, Y. Liu, Z. K. Zhang, F. Huang, Q. Tao, R. J. Ma, Y. L. An, L. Q. Shi, *Chem. Eur. J.* **2013**, *19*, 7437 – 7442; b) X. J. Liu, R. J. Ma, J. Y. Shen, Y. S. Xu, Y. L. An, L. Q. Shi, *Biomacromolecules* **2012**, *13*, 1307 – 1314.
[9] G. Y. Li, L. Q. Shi, R. J. Ma, Y. L. An, N. Huang, *Angew. Chem. Int. Ed.* **2006**, *45*, 4959 – 4962; *Angew. Chem.* **2006**, *118*, 5081 – 5084.
[10] a) Y. L. Wu, W. Chen, F. H. Meng, Z. J. Wang, R. Cheng, C. Deng, H. Y. Liu, Z. Y. Zhong, *J. Controlled Release* **2012**, *164*, 338 – 345; b) Y. Zhao, Y. X. Zhou, D. S. Wang, Y. J. Gao, J. W. Li, S. J. Ma, L. Zhao, C. Zhang, Y. Liu, X. R. Li, *Acta Biomater.* **2015**, *17*, 182 – 192; c) Q. Zhou, X. Guo, T. Chen, Z. Zhang, S. J. Shao, C. Luo, J. R. Li, S. B. Zhou, *J. Phys. Chem. B* **2011**, *115*, 12662 – 12670.
[11] a) Y. Q. Yang, W. J. Lin, L. J. Zhang, C. Z. Cai, W. Jiang, X. D. Guo, Y. Qian, *Macromol. Res.* **2013**, *21*, 1011 – 1020; b) W. J. Lin, S. Y. Nie, Q. Zhong, Y. Q. Yang, C. Z. Cai, J. F. Wang, L. J. Zhang, *J. Mater. Chem. B* **2014**, *2*, 4008 – 4020; c) D. Le Garrec, S. Gori, L. Luo, D. Lessard, D. C. Smit, M. A. Yessine, M. Ranger, J. C. Leroux, *J. Controlled Release* **2004**, *99*, 83 – 101; d) K. Ulbrich, V. Subr, *Adv. Drug Delivery Rev.* **2004**, *56*, 1023 – 1050.
[12] a) J. Jung, I. H. Lee, E. Lee, J. Park, S. Y. Jon, *Biomacromolecules* **2007**, *8*, 3401 – 3407; b) M. Lee, J. Jeong, D. Kim, *Biomacromolecules* **2015**, *16*, 136 – 144; c) Y. Q. Yang, L. S. Zheng, X. D. Guo, Y. Qian, L. J. Zhang, *Biomacromolecules* **2011**, *12*, 116 – 122; d) Z. F. Yuan, Z. Y. Que, S. Cheng, R. X. Zhuo, F. Li, *Chem. Commun.* **2012**, *48*, 8129 – 8131; e) L. Zhou, R. Cheng, H. Tao, S. B. Ma, W. W. Guo, F. H. Meng, H. Y. Liu, Z. Liu, Z. Y. Zhong, *Biomacromolecules* **2011**, *12*, 1460 – 1467; f) D. L. Wang, X. Y. Huan, L. J. Zhu, J. Y. Liu, F. Qiu, D. Y. Yan, X. Y. Zhu, *RSC Adv.* **2012**, *2*, 11953 – 11962; g) E. S. Lee, Z. Gao, Y. H. Bae, *J. Controlled Release* **2008**, *132*, 164 – 170.
[13] a) D. L. Wang, G. S. Tong, R. J. Dong, Y. F. Zhou, J. Shen, X. Y. Zhu, *Chem. Commun.* **2014**, *50*, 11994 – 12017; b) R. J. Dong, Y. F. Zhou, X. Y. Zhu, *Acc. Chem. Res.* **2014**, *47*, 2006 – 2016; c) R. J. Dong, Y. F. Zhou, X. H. Huang, X. Y. Zhu, Y. F. Lu, J. Shen, *Adv. Mater.* **2015**, *27*, 498 – 526.
[14] D. L. Wang, H. Y. Chen, Y. Su, F. Qiu, L. J. Zhu, X. Y. Huan, B. S. Zhu, D. Y. Yan, F. L. Guo, X. Y. Zhu, *Polym. Chem.* **2013**, *4*, 85 – 94.
[15] D. L. Wang, Y. Su, C. Y. Jin, B. S. Zhu, Y. Pang, L. J. Zhu, J. Y. Liu, C. L. Tu, D. Y. Yan, X. Y. Zhu, *Biomacromolecules* **2011**, *12*, 1370 – 1379.
[16] A. Bertrand, S. B. Chen, G. Souharce, C. Ladavière, E. Fleury, J. Bernard, *Macromolecules* **2011**, *44*, 3694 – 3704.
[17] H. H. Kuang, S. H. Wu, F. B. Meng, Z. G. Xie, X. B. Jing, Y. B. Huang, *J. Mater. Chem.* **2012**, *22*, 24832 – 24840.

Manuscript received: August 14, 2015
Accepted Article published: September 17, 2015
Final Article published: October 15, 2015